

Numerical continuation of bistable composite cylindrical shells

Alberto Pirrer MSc

PhD Student, Department of Aerospace Engineering, University of Bristol, UK

Daniele Avitabile PhD

Research Assistant, Department of Engineering Mathematics, University of Bristol, UK

Paul M. Weaver PhD

Professor, Department of Aerospace Engineering, University of Bristol, UK

Multi-stability of thin composite structures has shown potential for morphing applications. This paper, focusing on the bistability of composite cylindrical shells, aims to gather the analytical understanding to design bistability into shells and to define and study the parameters constraining their design envelope. A classic Rayleigh–Ritz method is used in conjunction with recently developed shell models taking into account curvature effects. A path-following method is used to solve the resulting non-linear set of equilibrium equations and to explore the design space. The method, which allows the capture of multiple stable and unstable equilibrium configurations, is benchmarked against finite-element computations.

1. Introduction

Interest in morphing structures has grown over recent years because of the advantages they can provide (Thill *et al.*, 2008). A structure that is able to change its shape and ‘tune itself’ to meet different operational requirements is attractive. With respect to aerospace structures, shape control of aerodynamic components can potentially offer significant improvements in performance. However, the subject is of general interest and can find applications in other engineering sectors.

One of the current aims of the structural engineering community is to gather the understanding to design materials and obtain tailored structural responses by exploiting the capabilities that anisotropy gives. In particular, this work seeks to establish the capabilities for analytical modelling and optimum design of novel composite structures that can achieve shape change by actuation from one stable state to another (i.e. bistability). Bistability may be designed into laminates such that the application of a threshold value of load or piezoelectric strain, for example, can achieve a controlled jump from one shape to another. The key feature for morphing applications is that, once in the alternative stable state, no energy or power is needed to maintain this shape.

Bistability of composite plates is now very well documented in literature (Cerami and Weaver, 2008; Hamamoto and Hyer, 1987; Mattioni *et al.*, 2008a). Conversely, bistability of other families of slender structures has not yet received the same attention. The current work relates to cylindrical shell structures. This paper presents a novel semi-analytical approach that allows one to define and study the design envelope of the latter (or in fact of any) family of structures. As a novel feature with respect

to previous works on bistable plates, the design space is explored in a systematic fashion by coupling a classic semi-analytical approach to numerical continuation software (Schilder, 2007).

The scope for potential applications will depend on the ‘shape’ of this design envelope, and the dedicated literature shows that both anisotropy and laminate shape may play an important role (Hyer, 1981; Seffen, 2007). A recently developed shell model (Pirrer and Weaver, 2009) that captures non-classical effects is used for analysis purposes.

2. Theoretical development and numerical solution

Cured flat, unsymmetric epoxy-matrix composite laminates will develop curvature when cooled to room temperature due to a mismatch in the thermal expansion behaviour of the layers within the laminate. In the early 1980s, an investigation into the room-temperature shapes of several families of unsymmetric laminates was conducted and it was noticed that they may not correspond to the prediction of classical lamination theory (Hyer, 1981). Instead of being a saddle shape as predicted by classical theory, many unsymmetric laminates may have two stable cylindrical shapes at room temperature. It was also observed that by applying a simple load, the structure could snap from one equilibrium to the other. Hyer (1981) incorporated geometric non-linearities into the classical theory to explain this behaviour. To correctly predict the room-temperature shapes of cross-ply laminates, Hamamoto and Hyer (1987) developed a non-linear approach based on polynomial approximations of the displacements and used a Rayleigh–Ritz minimisation of total potential energy. Following the aforementioned works, many researchers undertook studies

aiming to either deepen the physical insight and modelling abilities or find morphing-related applications (Cerami and Weaver, 2008; Diaconu *et al.*, 2008; Mattioni *et al.*, 2006, 2008a, 2008b, 2009).

An approach similar to that used by Hamamoto and Hyer (1987) is used here to investigate the bistability of unsymmetrically laminated cylindrical shells. It will involve the use of the novel shell model developed by Pirrera and Weaver (2009), which includes Qatu's (1999) recommendations on the effects of initial curvature on shells' anisotropy.

Equilibrium configurations are solutions to a set of non-linear algebraic equations deriving from the Rayleigh–Ritz minimisation. The resulting set of equations depends upon physical parameters such as the room temperature. In the current approach, the numerical solutions are continued in parameter space. That is, this work path follows equilibrium configurations as the control parameter varies, finds stable and unstable configurations, and detects bifurcations. The numerics are carried out using EPCont, a set of Matlab routines for numerical continuation (Schilder, 2007). The results are validated against finite-element analysis.

2.1 Problem definition

The aim is to investigate bistability of cylindrical composite panels with particular attention given to description of the solution procedure. In fact, this study is intended as a benchmark for the general solution technique. This procedure has been developed to be generally applicable to a whole set of bistability-related problems in such a way as to allow more general investigation into the design space of morphing bistable laminated structures.

The system to be analysed is essentially a cylindrical panel moulded with radius of curvature R and a square in-plane shape of side L . The panel is an unsymmetric laminate with stacking sequence $[0_2 90_2]$. The structure has free edges, is clamped in its central point and is subject to thermal load due to cooling from curing to room temperature. The engineering constants for graphite–epoxy (AS/3501) (Reddy, 2004) are shown in Table 1. Finite-element analyses show that this structure has two stable shapes at room temperature. These shapes will be found by using the Ritz method – that is, minimising a polynomial expansion of the total potential energy.

2.2 Total potential energy and shell model

Previous work has shown that some factors (e.g. anisotropy, laminate shape and geometrically non-linear deformations) may play a crucial role affecting the bistability of laminated composite structures and, consequentially, the design of morphing structures (Guest and Pellegrino, 2006; Hamamoto and Hyer, 1987; Iqbal and Pellegrino, 2000; Seffen, 2007). For this reason, use is made of the shell model developed by Pirrera and Weaver (2009). The model considers shells of general shape and takes into account all of the aforementioned factors. For current purposes, the model is specialised to cylinders. It is assumed that the middle surface of the shell structure is described by the curvilinear coordinate system (ξ_1, ξ_2, ζ) , where ξ_1 and ξ_2 are longitudinal and radial coordinates respectively (describing the position on the middle surface) and ζ is the coordinate in the thickness direction. This being the case, the principal radii of curvature are respectively $R_1 = \infty$ and $R_2 = R$. By assuming von Karman non-linearities and surface displacements to be

$$u(\xi_1, \xi_2, \zeta) = u_0(\xi_1, \xi_2) + \zeta\phi_1(\xi_1, \xi_2)$$

$$v(\xi_1, \xi_2, \zeta) = v_0(\xi_1, \xi_2) + \zeta\phi_2(\xi_1, \xi_2)$$

$$1. \quad w(\xi_1, \xi_2, \zeta) = w_0(\xi_1, \xi_2)$$

the non-linear strains are

$$2. \quad \begin{pmatrix} \varepsilon_1 \\ \varepsilon_2 \\ \varepsilon_4 \\ \varepsilon_5 \\ \varepsilon_6 \end{pmatrix} = \begin{pmatrix} e_1^0 + \zeta e_1^1 + \frac{1}{8}(e_5^0 - \kappa_2^0)^2 \\ \frac{e_2^0 + \zeta e_2^1}{1 + \zeta/R} + \frac{1}{8} \frac{(e_4^0 + \kappa_1^0)^2}{(1 + \zeta/R)^2} \\ \frac{e_4^0}{1 + \zeta/R} \\ e_5^0 \\ \omega_1^0 + \zeta\omega_1^1 + \frac{\omega_2^0 + \zeta\omega_2^1}{1 + \zeta/R} + \frac{1}{4} \frac{(e_5^0 - \kappa_2^0)(e_4^0 + \kappa_1^0)}{(1 + \zeta/R)} \end{pmatrix}$$

where

E_{11} : GPa	E_{22} : GPa	ν_{12}	G_{12} : GPa	G_{23} : GPa	α_1 : $10^{-6}/^\circ\text{C}$	α_2 : $10^{-6}/^\circ\text{C}$	t : mm
137.9	8.96	0.3	7.1	6.2	1.8	54	0.125

Table 1. Engineering constants for graphite-epoxy AS/3501

$$\begin{aligned}
 e_1^0 &= \frac{\partial u_0}{\partial \xi_1} & e_2^0 &= \frac{1}{R} \left(\frac{\partial v_0}{\partial \xi_2} + w_0 \right) \\
 \omega_1^0 &= \frac{\partial v_0}{\partial \xi_1} & \omega_2^0 &= \frac{1}{R} \frac{\partial u_0}{\partial \xi_2} \\
 e_4^0 &= \frac{1}{R} \left(\frac{\partial w_0}{\partial \xi_2} + R\phi_2 - v_0 \right) & e_5^0 &= \frac{\partial w_0}{\partial \xi_1} + \phi_1 \\
 \kappa_1^0 &= \frac{1}{R} \left(\frac{\partial w_0}{\partial \xi_2} - v_0 - R\phi_2 \right) & \kappa_2^0 &= -\frac{\partial w_0}{\partial \xi_1} + \phi_1 \\
 e_1^1 &= \frac{\partial \phi_1}{\partial \xi_1} & e_2^1 &= \frac{1}{R} \frac{\partial \phi_2}{\partial \xi_2} \\
 \omega_1^1 &= \frac{\partial \phi_2}{\partial \xi_1} & \omega_2^1 &= \frac{1}{R} \frac{\partial \phi_1}{\partial \xi_2}
 \end{aligned}$$

The total potential energy can then be written as (Reddy, 2004)

$$\begin{aligned}
 \Pi &= \int_{\Omega} \int_{-h/2}^{h/2} \left(\frac{1}{2} \boldsymbol{\varepsilon}^T \bar{\mathbf{Q}} \boldsymbol{\varepsilon} - \boldsymbol{\chi}^T \bar{\mathbf{Q}} \boldsymbol{\varepsilon} \Delta T \right) \\
 &\times R \left(1 + \frac{\zeta}{R} \right) d\zeta d\xi_1 d\xi_2
 \end{aligned}$$

where Ω denotes the mid-surface, h the thickness, ΔT the thermal load and $\bar{\mathbf{Q}}$ and $\boldsymbol{\chi}$ are the transformed stiffness matrix and the transformed thermal coefficient vector, respectively.

2.3 Polynomial approximation

The displacements are assumed to be

$$\begin{aligned}
 u_0(\xi_1, \xi_2) &= \sum_{m=0}^N \sum_{n=0}^m U_{n,m-n} \xi_1^n \xi_2^{n-m} \\
 v_0(\xi_1, \xi_2) &= \sum_{m=0}^N \sum_{n=0}^m V_{n,m-n} \xi_1^n \xi_2^{n-m} \\
 w_0(\xi_1, \xi_2) &= \sum_{m=0}^N \sum_{n=0}^m W_{n,m-n} \xi_1^n \xi_2^{n-m} \\
 \phi_1(\xi_1, \xi_2) &= \sum_{m=0}^N \sum_{n=0}^m X_{n,m-n} \xi_1^n \xi_2^{n-m} \\
 \phi_2(\xi_1, \xi_2) &= \sum_{m=0}^N \sum_{n=0}^m Y_{n,m-n} \xi_1^n \xi_2^{n-m}
 \end{aligned}$$

In other words, the displacements are approximated by a basis of complete polynomials truncated to order N . The coefficients $U_{n,m-n}$, $V_{n,m-n}$, $W_{n,m-n}$, $X_{n,m-n}$ and $Y_{n,m-n}$ are unknowns and, together with Equation 1, they uniquely define the displacements u , v and w . For the sake of simplicity, the same polynomial order

is used for all the displacement components, giving a total of $5(N+1)(N+2)/2$ unknowns. Nevertheless, by respecting the essential boundary conditions and imposing symmetries, this number can be reduced. In particular, the following conditions are enforced

- (a) u_0 and ϕ_1 are odd functions in ξ_1 and even functions in ξ_2
- (b) v_0 and ϕ_2 are even functions in ξ_1 and odd functions in ξ_2
- (c) w_0 is even in ξ_1 and ξ_2 , and it vanishes at the origin.

Plugging the resulting polynomial decomposition in Equation 4 and collecting all the unknown coefficients in a vector \mathbf{c} , the total potential energy is approximated by

$$\Pi \approx \Pi_N(\mathbf{c}, \Delta T)$$

which is now an algebraic function of the Lagrangian variables and temperature.

2.4 Solution technique and parameter continuation

For fixed ΔT , an equilibrium is a local extremum of the function Π_N . It is found by solving the system of non-linear algebraic equations

$$f_i(\mathbf{c}, \Delta T) = \frac{\partial \Pi_N}{\partial c_i} = 0, \quad i = 1, 2, \dots$$

$$\Leftrightarrow \mathbf{f}(\mathbf{c}, \Delta T) = 0$$

As stated already, the current aim is to explore the design space in a systematic fashion. In order to do so, a numerical continuation approach is used. Starting from $(\mathbf{c}_0, 0)$, the equilibrium solution for $\Delta T = 0$, it is possible to trace the locus of equilibria at different temperatures. This is done via a suitable parametrisation $(\mathbf{c}(s), \Delta T(s))$ passing by $(\mathbf{c}_0, 0)$ and satisfying

$$\mathbf{f}[\mathbf{c}(s), \Delta T(s)] = 0$$

The locus $[\mathbf{c}(s), \Delta T(s)]$ is called a solution branch. An advantage of numerical continuation is that it computes stable as well as unstable solutions, as long as they belong to the same solution branch. For instance, let us consider the bifurcation diagram presented by Hamamoto and Hyer (1987). For ΔT close to zero, the only solution is a saddle. At a critical temperature, the saddle becomes unstable and two other stable cylindrical solutions appear. A numerical simulation in which ΔT was varied quasi-statically would fail to compute the unstable saddle whereas, in the numerical continuation approach, stable and unstable saddles are computed naturally because they belong to the same solution branch $[\mathbf{c}(s), \Delta T(s)]$. Another immediate application in which such features would be useful is in tracing the non-linear force–

displacement diagram (complete with hysteresis) for a panel subject to snap-through.

In the present work, the expression for \mathbf{f} is computed symbolically via Maple 11. The resulting system of equations is exported as Matlab code and continued with EPCont. The results presented here concern only continuations in the parameter ΔT , but the proposed approach can be extended to any other design parameter (e.g. the radius of curvature or the side length).

3. Results

This section presents the numerical results obtained by continuing the system given by Equation 7 when $N = 5$, $L = 0.25$ m and $R = 0.5$ m. This polynomial order is a good compromise between accuracy and computational efficiency and it matches finite-element analysis adequately.

Figure 1 shows the continuation diagram for a cylindrical panel (i.e. $W_{2,0}$ and $W_{0,2}$ are plotted against the continuation parameter ΔT). From all of the Lagrangian coordinates, $W_{2,0}$ and $W_{0,2}$ were chosen as they are representative of the curvatures at the origin in the coordinate direction. As expected, the continuation diagram features two branches. The same diagram, on the other hand, shows the presence of three equilibria at room temperature, one of which is unstable.

The room-temperature equilibrium labelled 1 in Figure 1 is approximately a cylinder oriented as the moulded structure, but with greater curvature. Its shape is shown in Figure 2. For this solution, $W_{0,2}$ is large compared with $W_{2,0}$. Conversely, the equilibrium labelled 3, and shown in Figure 3, is a cylinder whose principal curvature is normal to that of the moulded panel ($W_{2,0}$ is large compared with $W_{0,2}$). Following solution 3 in parameter space along the branch to which it belongs, it was found that around $\Delta T = -40^\circ\text{C}$ the solutions become unstable via a saddle-node bifurcation. At $\Delta T = -180^\circ\text{C}$, a connected unstable equilibrium (labelled 2) was obtained, for which $W_{0,2}$ and $W_{2,0}$ are comparable. Notably, the stable solutions 1 and 3 are disconnected in parameter space.

The physical interpretation of this scenario is depicted in Figure 4. Starting from the cure temperature (labelled 0), the system follows the bottom branch until equilibrium 1. The reverse path is also possible. On the other hand, it is possible to start from equilibrium 3 on the solid part of the top branch and heat up the structure: after an initial deformation, the system will jump to the bottom branch and will eventually reach point 0. Conversely, equilibrium 3 will never be reached by simply cooling down from 0. In fact, an external intervention (i.e. an applied force) is necessary to make the structure snap onto the top branch and follow the equilibrium 3 branch.

Such a feature is particularly interesting as it is peculiar to initially curved panels. A similar behaviour was noted by Hamamoto and Hyer (1987); initially flat plates behave according

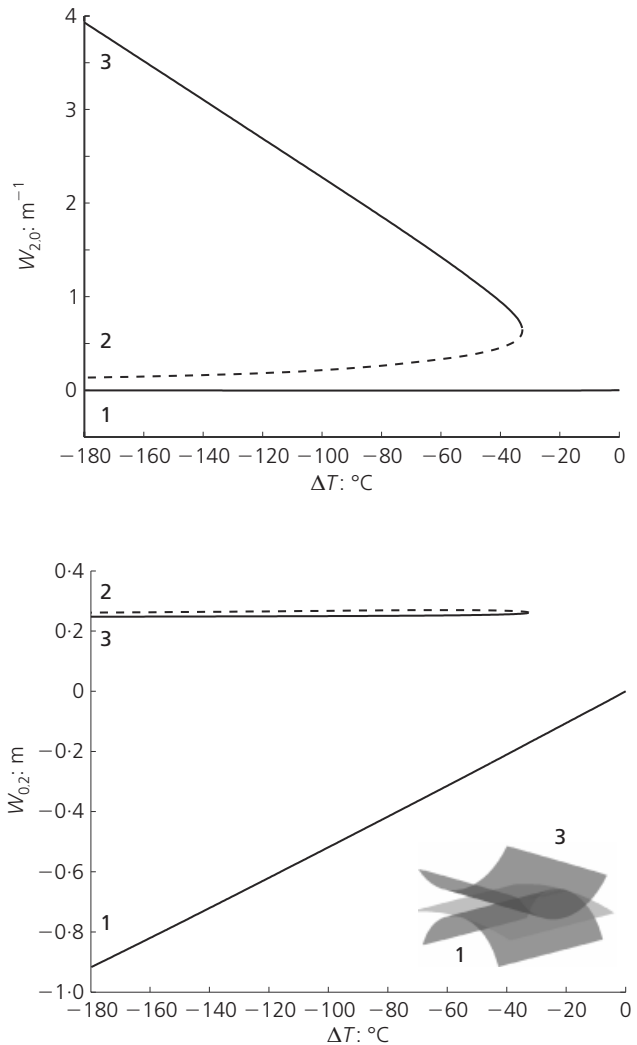


Figure 1. Bifurcation diagram: continuation from/to equilibria 1 and 3. Unstable branches are represented by dashed lines

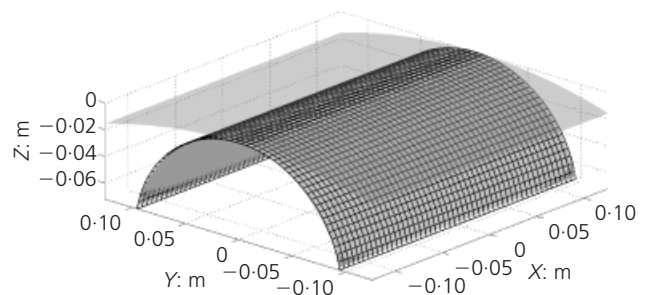


Figure 2. Equilibrium 1, finite-element analysis (solid surface) against analytical results (grid). Mould shape (equilibrium 0) on top

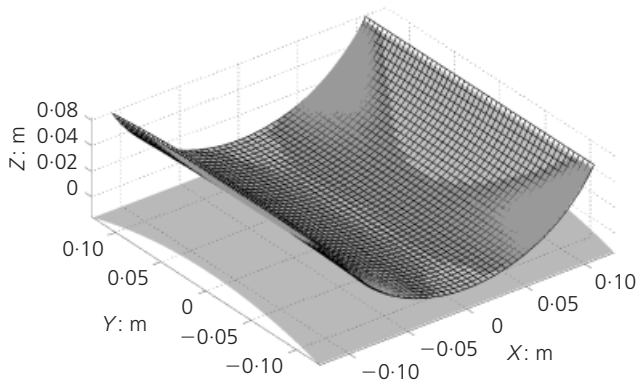


Figure 3. Equilibrium 3, finite-element analysis (solid surface) against analytical results (grid). Mould shape (equilibrium 0) on the bottom

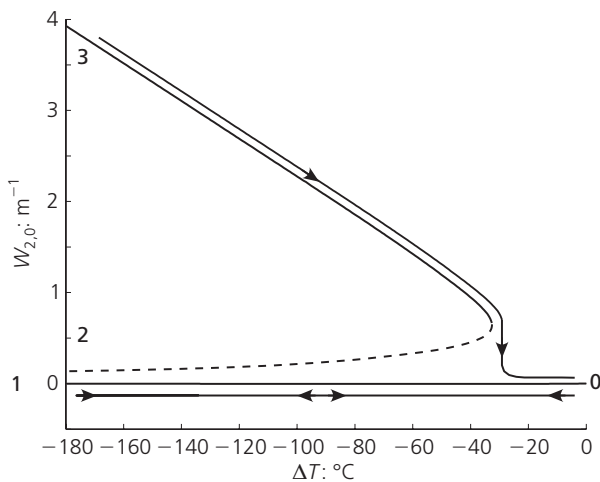


Figure 4. Bifurcation diagram and natural evolution of the system subject to temperature variations (line with arrows)

to the classical pitchfork scenario: equilibria analogous to 1 and 3 can be followed from point 0 and vice versa. Imperfect plates, on the other hand, behave accordingly to Figure 4.

The code was benchmarked against finite-element simulations performed with the commercial software Abaqus. The panel was modelled using 1764 four-node-square shell elements (S4R) with a total of 1849 nodes. Mesh refinement studies showed that the chosen mesh density, given acceptable computational time, gave sufficiently accurate results; indeed, further mesh refinement gave a negligible change in results. The cool-down and snap-through processes were simulated by using ‘Static, General’ steps with ‘Nlgeom’ on. When convergence was difficult to achieve, use was made of the option ‘stabilization with: dissipated energy fraction’. This option makes the simulation pseudo-dynamic by adding fictitious viscous forces to damp instabilities and improves the convergence properties of the system. This allows the structure to

jump to the different branches of the solution as indicated by the line with arrows in Figure 4.

A comparison of the stable shapes obtained with both methods (Figures 2 and 3) shows excellent agreement. The approach proposed here matches finite-element analysis precision with a substantially smaller amount of unknowns. This is largely due to the fact that the polynomial expansions (Equation 5) are already a good guess of the possible solutions.

Figures 5 to 8 analyse in better detail convergence of the proposed method with finite-element analysis. If u is the displacements obtained in Cartesian coordinates with the continuation methods and u_{FE} the corresponding finite-element displacements, the scalar error e can be defined as

$$9. \quad e(x, y) = \|u(x, y) - u_{FE}(x, y)\|$$

Figures 5 and 7 show the cross-section errors $e(0, y)$ and $e(x, 0)$ for equilibria 1 and 3 respectively. Figures 6 and 8 show $e(x, y)$ for the full panel. The achieved tolerance is always below 10^{-3} , which is accurate in view of the degrees of freedom employed in the calculation.

4. Conclusions and future work

This work has developed a methodology for systematic investigation of bistability-related problems. As a test case, the bistability of a cylindrical panel was studied. The work adopted the shell theory proposed by Pirrer and Weaver (2009), which takes into account features that are found to play a fundamental role in bistability problems. A comparison of the results obtained by using this theory and other classical theories is beyond the scope

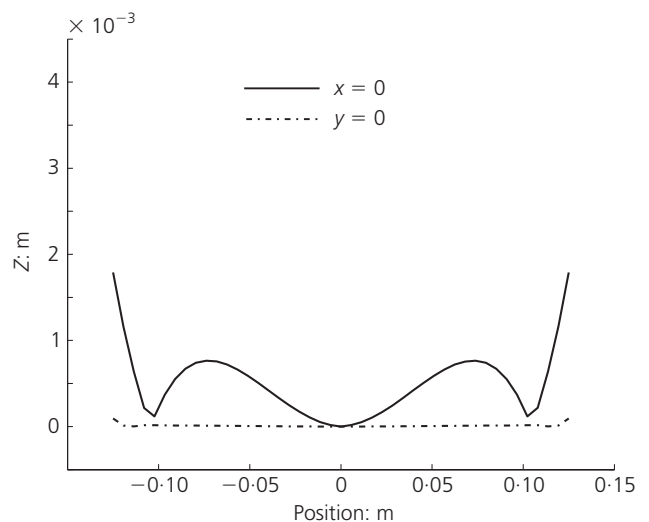


Figure 5. Equilibrium 1: norm of the difference between finite-element analysis and model results along the middle sections (dimensions in metres)

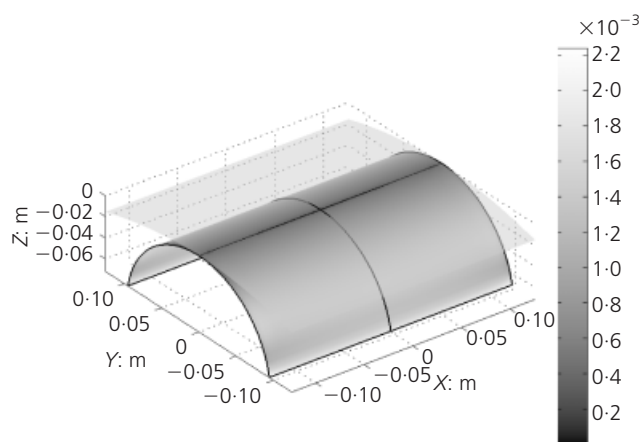


Figure 6. Equilibrium 1: norm of the difference between finite-element analysis and model results. The scale bar refers to the error $e(x, y)$ (dimensions in metres)

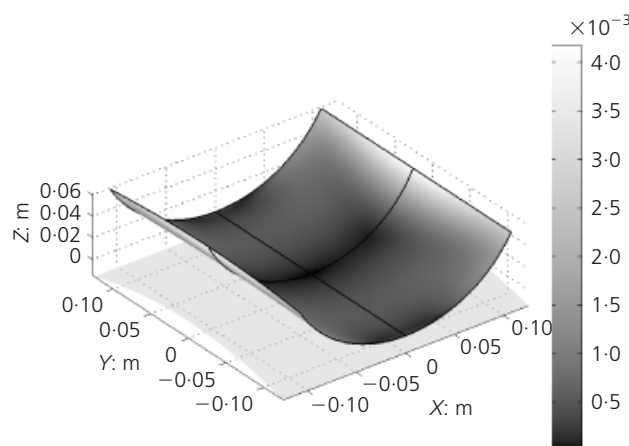


Figure 8. Equilibrium 3: norm of the difference between finite-element analysis and model results. The scale bar refers to the error $e(x, y)$ (dimensions in metres)

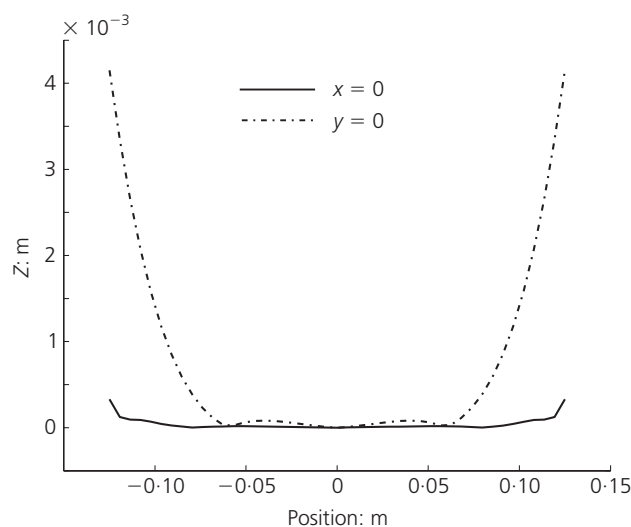


Figure 7. Equilibrium 3: norm of the difference between finite-element analysis and model results along the middle sections (dimensions in metres)

of this paper. However, it is noted that adoption of this theory led to good agreement with finite-element results. The behaviour of a cylindrical panel subject to thermal load was characterised. The system showed peculiarities (i.e. the broken pitchfork continuation diagram) that make it different from previously studied bistable systems such as cured flat plates.

Continuation methods were used to explore the design space, and the behaviour of the structure subject to temperature variations was studied. This approach can, however, be extended to other design parameters such as in-plane shape, radius of curvature of the mould or applied load. Relevant results will be provided in the future.

Acknowledgements

The authors acknowledge funding from Airbus UK and SWRDA through a Great Western Research grant. Dr Avitabile thanks the EPSRC for funding the ‘Making it Real’ grant.

REFERENCES

- Cerami M and Weaver PM (2008) Characterization of unsymmetric cross-ply laminate deflections using orthogonal polynomials. *Proceedings of the 49th AIAA/ASME/ASCE/AHS/ASC Structures, Structural Dynamics, and Materials Conference, Schaumburg, IL*. AIAA, Reston, VA, paper 2008-1928.
- Diaconu CG, Weaver PM and Mattioni F (2008) Concepts for morphing airfoil sections using bi-stable laminated composite structures. *Thin-Walled Structures* **46**(6): 689–701.
- Guest SD and Pellegrino S (2006) Analytical models for bistable cylindrical shells. *Proceedings of the Royal Society A Mathematical Physical and Engineering Sciences* **462**(2067): 839–854.
- Hamamoto A and Hyer MW (1987) Nonlinear temperature–curvature relationships for unsymmetric graphite-epoxy laminates. *International Journal of Solids and Structures* **23**(7): 919–935.
- Hyer MW (1981) Calculations of the room-temperature shapes of unsymmetric laminates. *Journal of Composite Materials* **15**(7): 296–310.
- Iqbal K and Pellegrino S (2000) Bi-stable composite shells. *Proceedings of the 41st Aiaa/Asme/Asce/Ahs/Asc Structures, Structural Dynamics, and Materials Conference and Exhibit, Atlanta, GA*. AIAA, Reston, VA, paper 2000-1385.
- Mattioni F, Weaver PM, Potter K and Friswell MI (2006) Multi-stable composites application concept for morphing aircraft. *Proceedings of the 16th International Conference on Adaptive Structures and Technologies, Paris, France*. Destech Publications, Lancaster, PA, pp. 45–52, 401.

-
- Mattioni F, Weaver PM, Potter K and Friswell MI (2008a) Analysis of thermally induced multistable composites. *International Journal of Solids and Structures* **45(2)**: 657–675.
- Mattioni F, Weaver PM, Potter K and Friswell MI (2008b) The application of thermally induced multistable composites to morphing aircraft structures. *Proceedings of SPIE* **6930**: 93012.
- Mattioni F, Weaver PM and Friswell MI (2009) Multistable composite plates with piecewise variation of lay-up in the planform. *International Journal of Solids and Structures* **46(1)**: 151–164.
- Pirrerá A and Weaver PM (2009) Geometrically nonlinear first-order shear deformation theory for general anisotropic shells. *AIAA Journal* **47(3)**: 767–782.
- Qatu MS (1999) Accurate equations for laminated composite deep thick shells. *International Journal of Solids and Structures* **36(19)**: 2917–2941.
- Reddy JN (2004) *Mechanics of Laminated Composite Plates and Shells: Theory and Analysis*, 2nd edn. Boca Raton, FL, CRC Press.
- Schilder F (2007) EPCont: a continuation toolbox for Matlab. Personal communication.
- Seffen KA (2007) ‘Morphing’ bistable orthotropic elliptical shallow shells. *Proceedings of the Royal Society A Mathematical Physical and Engineering Science* **463(2077)**: 67–83.
- Thill C, Etches J, Bond I, Potter K and Weaver P (2008) Morphing skins. *Aeronautical Journal* **112(1129)**: 117–139.

WHAT DO YOU THINK?

To discuss this paper, please email up to 500 words to the editor at journals@ice.org.uk. Your contribution will be forwarded to the author(s) for a reply and, if considered appropriate by the editorial panel, will be published as a discussion in a future issue of the journal.

Proceedings journals rely entirely on contributions sent in by civil engineering professionals, academics and students. Papers should be 2000–5000 words long (briefing papers should be 1000–2000 words long), with adequate illustrations and references. You can submit your paper online via www.icevirtuallibrary.com/content/journals, where you will also find detailed author guidelines.